Evaluating the quality of 4D warping and time-shift estimation using cross-correlation and dynamic time warping

Vinicius Lemos de Almeida*[1], Marcella Rapini Braga[1], Fernando Sergio de Moraes[2], Allan Peixoto de Franco[2] and Vitor Leal de Mello[1], [1] Petrobras, [2] UENF

This paper was prepared for presentation during the 17th International Congress of the Brazilian Geophysical Society held in Rio de Janeiro, Brazil, 16-19 August 2021.

Abstract

In this work, we present a comparison between two methods for estimating 4D time-shifts: cross-correlation and dynamic time warping. Getting a good time-shift correction is essential to produce reliable 4D amplitude and impedance differences. More than that, time-shifts are also a complementary attribute for interpretation. By using synthetic models, we investigate the impact of input data sample rate, time window length and frequency filtering to the quality of time-shift prediction and post-warping data. Both methods proved to be reliable. However, the Dynamic Time Warping show superior accuracy in the presence of noise and for large time-shifts. Additionally, we demonstrate that applying frequency filtering increases the 4D repeatability.

Introduction

4D seismic is a technique which compares two or more 3D seismic data acquired on different dates in order to monitor changes in reservoir and surrounding rocks caused by production. The oldest survey is called baseline seismic and the following are called monitors. The success of a 4D seismic monitoring project depends on the detectability and repeatability factors. The detectability is related to the magnitude of changes on physical properties, which is controlled by the rock and fluid characteristics and depletion process. The repeatability, represent the level of similarity between acquisition geometry / parameters and the seismic processing steps (Johnston, 2013).

The goals of a 4D processing differ from usual 3D workflows and therefore demand additional steps. requires. The 4D warping is one of them and consists of aligning equivalent events in monitor data with respect to the baseline seismic. This correction is an essential step prior to the interpretation of amplitude changes and is applied using a time-shift cube . The time-shift itself is also an important interpretation tool, as it can indicate pressure variations, saturation changes, and geomechanical effects (within and outside the reservoir). The increasing importance of time-shifts in 4D interpretation has given rise to a number of methods, such as those based on cross correlation (Rickett and Lumley 2001; Hale, 2006), Taylor series approximations (Hatchell et al. 2003), waveform inversion (Rickett et al. 2007), dynamic programming (Hale, 2009) and image consistency (Thore et al. 2012). Among these methods, the cross-correlation (CC) is the most popular, it is robust and easy to implement, as shown in Rickett and Lumley (2001) and Hale (2006), but it is necessary to determine windowing parameters. An alternative to avoid sliding windows is the Dynamic Time Warping (DTW). This solution originally emerged in the speech recognition context (Sakoe and Chiba, 1978) and an application for 4D warping purposes was presented by Hale (2012). The DTW imposes restrictions on which shifts may vary over time. These constraints generally allow DTW to estimate accurate shifts between signals that are noise-contaminated or are not simply deformed versions of the other (Hale, 2013).

The present work aims to identify the best practices in the application of DTW and CC techniques, and to compare such methods using 4D synthetic seismic models since comparisons between time-shift calculation techniques are not systematic in the literature.

Method 1: Cross-correlation

The use of cross-correlation is very common in the seismic universe, being applied to a multitude of processes, including noise attenuation (Abma and Claerbout, 1995; Güulunay, 2000), interpolation of missing samples (Crawley et al., 1999), corrections of differences in seismic acquisition and processing, (Rickett and Lumley, 2001) as well as in 4D time-shift calculation (Hale, 2012).

The use of cross-correlation methods implies that a sliding window is required, where the lag associated to the maximum correlation coefficient within each window represents the local time-shift between two traces. The discrete version of the cross-correlation (c) equation is:

$$c[v] = (B * M)[v] \equiv \sum_{j=-\infty}^{\infty} B[j]M[j+v], \qquad (1)$$

Where v is the cross-correlation lag, B is the baseline trace and M the monitor trace.

To obtain a local cross-correlation, we apply a smooth Gaussian window function for each trace B and M before calculating the cross-correlation.

Considering now the process of local cross-correlation and sliding the Gaussian window to the right or left, a different local cross-correlation is obtained. In fact, one can calculate the local cross-correlation window for each of the samples of baseline and monitor traces to obtain the time-shift.

Method 2: Dynamic Time Warping (DTW)

DTW is a technique that uses a dynamic programming approach to align two time series so that a distance measurement between series is minimized (Berndt and Clifford, 1994). In this work an algorithm was implemented to calculate the time-shift between two time series using the Dynamic Time Warping method, following the concepts presented in Hale (2013) and Caparica (2014).

Baseline and monitor seismic traces are represented as two time series, B and M, respectively, with n elements:

$$\mathrm{B} = b_1, b_2, \dots, b_n \quad and \quad \mathrm{M} = m_1, m_2, \dots, m_n. \tag{2}$$

Thus, the time series can be related by M [n] = B [n + s [n]], where s [n] is the time-shift. B and M can be represented on a Cartesian plane, forming a matrix of dimensions n x n, where each element (i, j) represents the closeness between the series elements. Elements (i, I) are an image of alignment errors between time sequences, and they can be measured in different ways as shown by Berndt and Clifford (1994):

$$\begin{gathered} \mathrm{e}(i,l) = |\, M(i) - B(i+l)| \\ or \\ e(i,l) = |M(i) - B(i+l)|^2 \end{gathered} \tag{3}$$

only the quantification of the proximity between the two series is important.

The time warp problem computes a sequence of integer time-shifts u [0: N - 1], solving the following problem, Hale (2013):

$$\mathrm{u}[0\colon \mathrm{N}-1] = argmin_{[0:N-1]} D(l[0\colon N-1]) \tag{4}$$

where,

$$D(l[0\colon N-1]) \approx \sum_{i=0}^{(N-1)} e[i, l(i)]. \tag{5}$$

Being l the strain path that best aligns the sequences $B(i+l)$ and $M(i)$, so that the distance function (D) is minimized.

The problem is subject to the restrictions to prevent the sequence from changing too rapidly from one sample to the next and to define the distortion window width, in order to improve the algorithm performance and stablish the maximum time-shift between sequences as shown by Hale (2013). The sequence u is an approximation of the time-shifts s acquired by applying the Dynamic Time Warping (DTW) method.

Synthetic Models

We generated a baseline trace using sonic and density logs of a given well from the Marlim Field in Campos basin, Rio de Janeiro. Then, we used the baseline as a reference for modeling three monitor scenarios:

Monitor 1: represents exactly the baseline trace warped by a sinusoidal time-shift function and aims to achieve the maximum time-shift variations commonly found in real cases (approximately 10ms) (Figure 1);

Monitor 2: is a noisy version of Monitor 1. In this scenario we assume the noise amplitude as 10% of maximum signal amplitude (Figure 1);

Monitor 3: simulates a velocity perturbation at reservoir level due to pressure/saturation changes and aims to evaluate the effectiveness of both methods in the presence of amplitude variations, as expected in the reservoir (Figure 3).

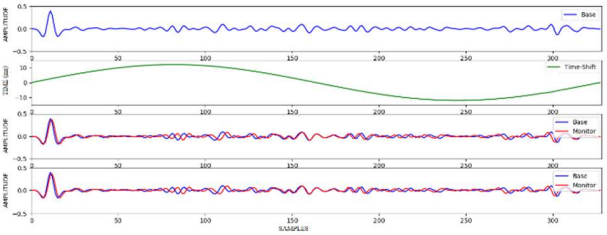

Figure 1: Baseline amplitude trace generated through sonic and density well logs; a sinusoidal time-shift in milliseconds, and; a comparison between baseline and monitor 1, and; comparison between baseline and monitor 2.

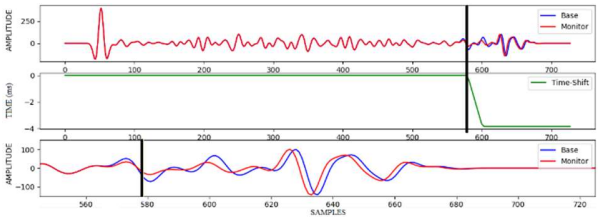

Figure 2: A comparison between baseline amplitude trace and the monitor 3; the theoretical time-shift in milliseconds, and; baseline and monitor 3 within reservoir interval highlighted. The black line indicates the top of the reservoir where non-zero time-shifts start to appear.

Note that, the baseline and monitor 3 show a detachment before the top of the reservoir in disagreement with the theoretical time-shifts (Figure 2). This effect is a consequence of the wavelet side lobes because reflectivities are different in the baseline and monitor traces. False effects arising from the application of time-shift in amplitude data are shown by Griffiths et al. (2015). To evaluate the differences in time-shift estimates in amplitude and impedance data, the baseline and monitor 3 P-impedances were generated (Figure 3).

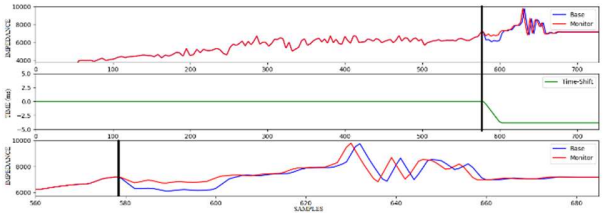

Figure 3: The baseline and monitor 3 P-impedance traces; theoretical time-shift, and; baseline and monitor traces

within reservoir interval highlighted. The black line indicates the top of the reservoir where non-zero time-shifts start to appear.

Results

In this step the objective is to test the efficiency of the Dynamic Time Warping and Cross-Correlation methods in the time-shift calculation. Comparisons were made between calculated and expected time-shifts and the consequences generated on post-warping amplitude and impedance differences (monitor - baseline).

Time-shifts estimation

In this step the time-shifts for both monitor scenarios were calculated using the Dynamic Time Warping (DTW) and Cross-Correlation (CC) methods with different sample rates, window lengths and smoothing parametrizations. The purpose of these examples is to observe the effect of signal sample rate on DTW and sliding window size on cross-correlation time-shifts.

For the time-shift calculation, we applied the DTW method to synthetic traces resampled to 1, 2 and 4 ms. For the CC method we chose time windows lengths of 21, 41 and 61 samples (data sampled at 4ms), which are equivalent to a window of 84, 164 and 244 ms, respectively. We measured the similarity between the true and the calculated time-shift through the NRMS, as shown in the Figure 4.

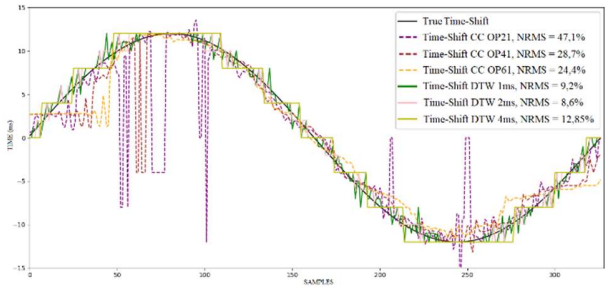

Figure 4: Time shift calculated using the DTW method, with 1, 2 and 4 ms sampling, and the CC method with window of 21, 41 and 61 samples for the monitor 1 (noise-free).

The dashed lines show the CC results while continuous lines the DTW results. Figure 4 shows lower NRMS values when time-shifts are calculated by the DTW method. Analyzing each method separately, it is possible to verify that the NRMS consistently decreases as sample rate increase in DTW and window length increase in CC. The obtained NRMS are: 47%, 29% and 24% for CC and 12%, 9% and 9% to DTW. Also, time-shifts calculated using the cross-correlation method show misalignment at the beginning and the end of non-zero time-shifts. These undesirable effect increases for longer sliding windows. The results presented in Figure 4, makes evident the need to test some filtering types in order to smooth the final time-shift. High Frequency Cutoff (SCAF) smoothing has been tested and the best result is shown in Figures 5.

Evaluating Figure 5, it can be stated that the DTW method, followed by smoothing was able to reconstruct the time-shift trend satisfactorily in all samples for the noiseless monitor trace. More than that, the repeatability increases. Final NRMS are 8%, 4% and 3%. The CC method proves to be less stable, especially at intervals where the time-shift reaches higher values or curvature. Final CC NRMS are 30%, 21% and 23%. In these cases, there is also a misalignment at the beginning and the end of the trace that increases with the window size.

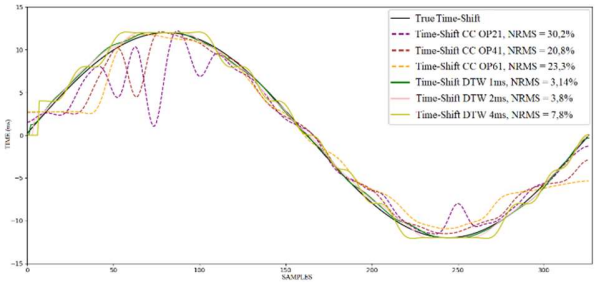

Figure 5: Time-shift calculated using the DTW method, with 1, 2 and 4 ms sampling and CC with windows of 21, 41 and 61 samples for the monitor 1. All with smoothing cuts high at 25 Hz frequency (SCAF).

In Figure 6 we repeated the procedure applied in Figure 4 but using monitor 2. It shows the time-shifts and the NRMS values obtained by the DTW method. Note that the NRMS increase substantially in the presence of noise, ranging from 17 to 19%, even though always better than CC (24 to 51%)

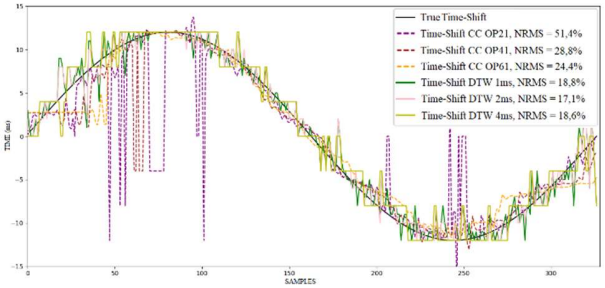

Figure 6: Time-shift calculated using the DTW method, with 1, 2 and 4 ms sampling, and the CC method with a window of 21, 41 and 61 samples for the monitor 2 (10% noise).

In the DTW method it is possible to verify that with the addition of the noise the NRMS values are closer in the different samplings used. On the other hand, a clear relationship between window length and NRMS is observed in CC. The larger the windows, the lower the NRMS values, but misalignments at the beginning and the end of time-shifts traces continue to increase along with window size.

Figure 7 shows the results for monitor 2 after the application of 25Hz SCAF. By applying smoothing, the NRMS values decrease significantly for the time-shifts calculated by both methods: 7 to 9% for DTW and 20 to 34% for CC. For monitor 2, smoothed DTW with 1 and 2ms samples rates provided the best approximations of the true time-shifts, confirming the relationship between sampling and accuracy for DTW.

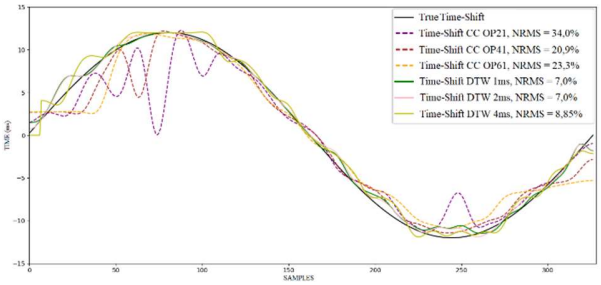

Figure 7: Time-shifts calculated using the DTW method, with 1, 2 and 4 ms sampling, and the CC method with 21, 41 and 61 samples window for the monitor 2 (10% noise), all with 25Hz SCAF.

For the comparisons using monitor 3 we limited the DTW application on sample rates of 1 and 2 ms sampling, and for cross-correlation we kept the window sizes of 21, 41 and 61 samples. Figure 8 shows the results of time-shift calculated in amplitude traces zoomed in the region near the top of the reservoir. Being both DTW and CC methods applied with 25Hz SCAF.

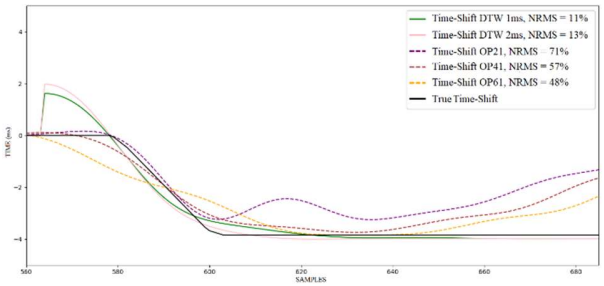

Figure 8: Time-shift calculated in amplitude traces using the methods DTW (1 and 2 ms sampling) and cross-correlation (window with 21, 41 and 61 samples), with 25Hz SCAF.

The results from Figure 8 show a better estimate of the true time-shift within the reservoir using the 41-sample window cross-correlation method, but the method finds instability when the time-shift analysis passes through the reservoir. Focusing at the NRMS values, it is clear that when considering the full trace, the DTW method for 1 ms has the best results, even though it is more sensitive to the wavelet effect above the top of reservoir.

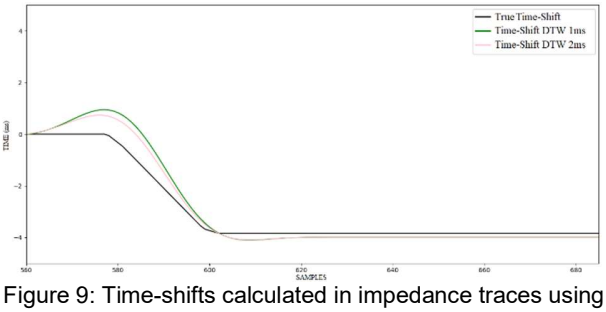

Figure 9: Time-shifts calculated in impedance traces using the method DTW (1ms and 2ms sampling), with 25Hz SCAF.

In Figure 9, the time-shift was calculated by the DTW method using the impedance traces as input. Comparing the time-shift estimates calculated by the DTW method for amplitude (Figure 8) and impedance (Figure 9), some relevant differences can be observed, which can possibly impact the amplitude and impedance 4D difference traces.

Amplitude and Impedance Differences After Warping

In this section we focus on the analysis of the quality of amplitude and impedance 4D differences traces. This step it is not only necessary for 4D interpretations, but it is also a good quality control by the processing perspective. The interpolations applied to the monitor and the warping process application might generate amplitudes changes. Thus, even applying warping with true time-shift, the difference between monitor and baseline will not be zero, thus generating residual differences. To facilitate the analysis, the difference between the baseline and the residuals generated by the interpolation were subtracted from the amplitude differences. Time-shifts from both DTW and CC methods with 25Hz SCAF smoothing were the input to the warping processes, since the approach with smoothing presents superior results on the previous examples. Figure 10 show the resulting post-warping amplitude difference traces.

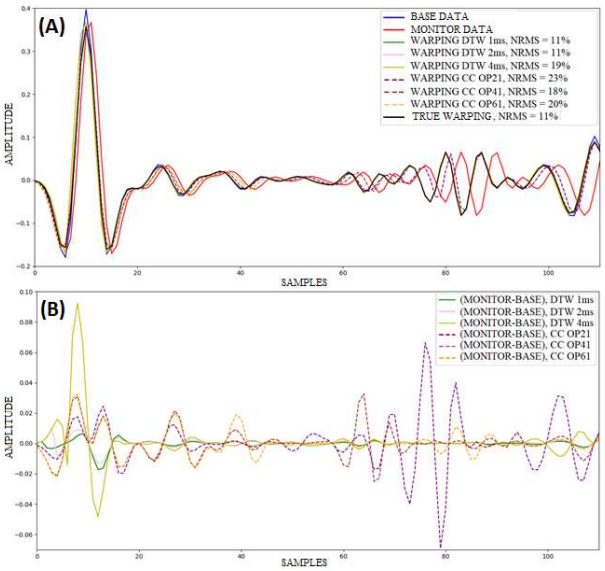

Figure 10: (A) Region between samples 0 and 110 of the baseline, monitor and time-shift corrected monitor data by the DTW and CC methods with 25Hz SCAF application. (B) Amplitude difference between time-shift corrected monitor and baseline.

The DTW method for 1 and 2 ms sample rates, followed by smoothing, aligned the monitor data to the baseline over the complete trace, making the amplitude difference close to zero after the residue subtraction. DTW with 4ms sampling failed to correct the monitor at some points generating amplitude differences that could result in misinterpretations. The cross-correlation method proved to fail on the correct alignment, especially in regions where time-shifts are large, which also may lead to errors in

interpretation. In regions with lower values the CC method works properly.

Figure 11 shows the post-warping monitor data with random noise and the resulting amplitude differences. Both methods are effective with noise, presenting acceptable NRMS values for the presented noise level. However, false amplitude differences above the noise level are perceived using both DTW and CC methods. Analyzing the examples of the monitor 2 it can be stated that the DTW and CC methods can satisfactorily align monitor and baseline data in the regions with the low time-shift variations. However, when the variations are high, DTW produce better results than the cross-correlation.

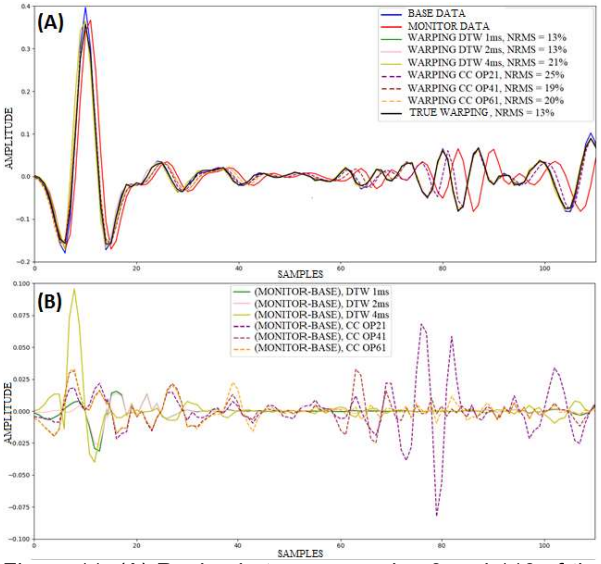

Figure 11: (A) Region between samples 0 and 110 of the baseline, monitor with 10% noise and time-shift corrected monitor data by the DTW and CC methods with 25Hz SCAF application. (B) Amplitude difference between time-shift corrected monitor and baseline.

Working with seismic data with high signal to noise ratio is of paramount importance for good interpretation. The examples shown above confirm that from certain noise levels 4D anomalies can be confused with noise. Figure 12 shows the results obtained by applying the time-shift calculated by both DTW and cross-correlation methods on the monitor data for the monitor 2. Warping using the time-shift calculated by the DTW and CC methods has reached NRMS values very similar to those applied by the true time-shift. However, there is a slight misalignment at the beginning of the data with warping applied using the DTW method and a small misalignment throughout using the CC method. The effects of these small misalignments can be seen in the differences in amplitude between the monitor and baseline data.

In both methods it is possible to accurately mark the top (sample 578) and bottom (sample 605) of the reservoir, but the DTW method, as seen in Figure 12, yield amplitude differences closest to the expected and generating fewer artifacts compared to the CC method.

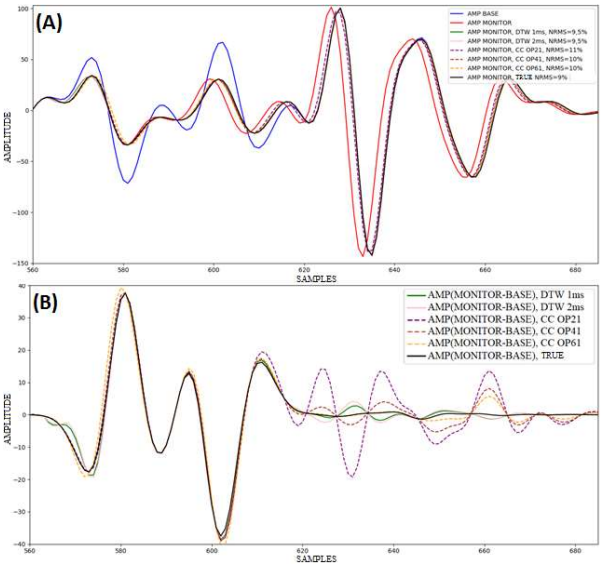

Figure 12: (A) Region between samples 560 and 700 of the baseline, monitor and time-shift corrected monitor data by DTW and CC methods with 25Hz SCAF application. (B) Amplitude difference between time-shift corrected baseline and monitor.

To investigate the impact of warping the impedance trace, the monitor data was corrected with the time-shifts generated from the DTW method in the amplitude and impedance data. The impedance differences between the warped monitor and baseline data are shown in Figure 13. The artifact above the top of the reservoir in the impedance difference trace, Figure 13, is more pronounced when the time-shift is calculated in amplitude. This effect is associated with the error in the time-shift estimation caused by the wavelet influence.

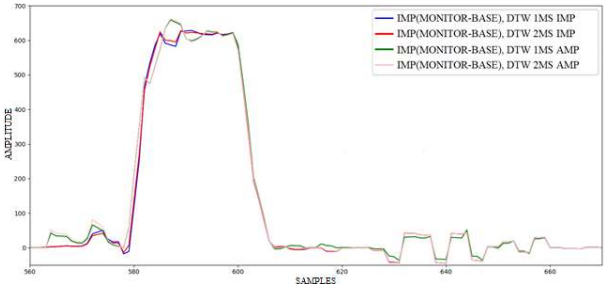

Figure 13: Region between samples 560 and 700 of the impedance difference between baseline and warped monitor by DTW methods calculated on amplitude and impedance traces and subsequently applied the 25Hz SCAF.

Conclusions

Supported by synthetic models important observations allowed us to increase confidence in the calculation of the time-shift by the Dynamic Time Warping and cross correlation methods. The methods showed greater accuracy when smoothed by frequency filters. Comparing with cross correlation, the Dynamic Time Warping was more accurate in all scenarios covered in this study:

presence of noise or amplitude variation between monitor and baseline data (simulating 4D signal).

The simulated noise affected the post-warping 4D differences, creating false anomalies. These undesirable effects are more pronounced when the time-shift is calculated using the cross-correlation method. When amplitude changes are superimposed to the time-shifts, the effect of the wavelet at the top of the reservoir creates some artifacts. The Dynamic Time Warping method proved to be more sensitive to this effect, although the better accuracy in the warping process. In this example we also tested the application of the warping on the impedance traces. It reveals that amplitude derived time-shifts applied to impedance traces gives rise to false anomalies above the top of the reservoir in the impedance difference trace.

Acknowledgments

The authors thank ANP for authorizing this publication as well as Petrobras and UENF for supporting this research.

References

Abma, R., and Claerbout, J., 1995, Lateral prediction for noise attenuation by t-x techniques: Geophysics, v. 60, no. 6, p. 1887-1896.

Berndt, D. J. Clifford, J., 1994. Using dynamic time warping to find patterns in time series. In:KDD Workshop'94. [S.l.: s.n.], 1994. p. 359–370.

Caparica, J., 2014. Uma metodologia eficiente para inversão de avo multicomponente. (Master dissertation, Universidade Estadual do Norte Fluminense).

Crawley, S., Clapp, R., and Claerbout, J., 1999, Interpolation with smoothly non-stationary prediction-error filters: 69th Annual International Meeting, SEG, Expanded Abstracts, p. 1154-1157.

Griffiths, L., Blanchard, T.D., Edgar, J.A. and Shahraeeni, M.S., 2015, June. Trace Warping vs. Impedance Warping in 4D Seismic Inversion. In 77th EAGE Conference and Exhibition 2015.

Gulunay, N., 2000, Noncausal spatial prediction filtering for radom noise reduction on 3-D poststack data: Geophysics, v. 65, no. 5, p. 1641-1653.

Hale, D., 2006, Fast local cross-correlations of images: 76th Annual International Meeting, SEG, Expanded Abstracts, 3160–3164.

Hale, D., 2009, A method for estimating apparent displacement vectors from time-lapse seismic images: Geophysics, 74, P99–P107. Hall, S., 2006, A methodology Hale, D., 2012. An efficient method for computing local cross-correlations of multi-dimensional signals: Center for Wave Phenomena, Colorado School of Mines, Golden CO 80401, USA.

Hale, D., 2012. An efficient method for computing local cross-correlations of multi-dimensional signals: Center for Wave Phenomena, Colorado School of Mines, Golden CO 80401, USA.

Hale, D., 2013. Dynamic warping of seismic images: Center for Wave Phenomena, Colorado School of Mines, Golden CO 80401, USA.

Hatchell P. J., Vanden Beukel A., Molenaar M. M., MaronK.P., Kenter C.J., Stammeijer J.G.F., et al., 2003. Whole earth 4D: reservoir monitoring geomechanics. 73rd SEG Annual Meeting, Dallas, TX, Expanded Abstracts, 1330–1333.

Johnston, D. H., 2013. Practical applications of time-lapse seismic data. Society of Exploration Geophysicists.

Rickett, J. E., and D. E. Lumley, 2001, Cross-equalization data processing for time-lapse seismic reservoir monitoring: A case study from the Gulf of Mexico: Geophysics, 66, 1015–1025.

Rickett J., Duranti L., Hudson T., Regel B. and Hodgson N., 2007.4D time strain and the seismic signature of geomechanical compaction at Genesis. The Leading Edge 26, 644–647.

Sakoe and Chiba, 1978. Dynamic Programming Algorithm Optimization for Spoken Word Recognition. IEEE Transactions on Acoustics, Speech, and Signal Processing, Vol. Assp-26, no. 1, February 1978.

Thore, P., de Verdiere, C. and McManus, E., 2012. Estimation of 4D signal in complex media, A fast track approach. 82nd Annual International Meeting, SEG, Expanded Abstracts.